Release of Oxygen from Copper Oxide Cluster Ions by Heat and by Reaction with NO

ARTICLE *in* THE JOURNAL OF PHYSICAL CHEMISTRY C · FEBRUARY 2015

Impact Factor: 4.77 · DOI: 10.1021/jp511840d

3 AUTHORS, INCLUDING:

Ken Miyajima
The University of Tokyo
54 PUBLICATIONS **1,154** CITATIONS

SEE PROFILE

THE JOURNAL OF PHYSICAL CHEMISTRY C

Article

pubs.acs.org/JPCC

Release of Oxygen from Copper Oxide Cluster Ions by Heat and by Reaction with NO

Fumitaka Mafuné,* Ken Miyajima, and Keisuke Morita

Department of Basic Science, School of Arts and Sciences, The University of Tokyo, Komaba, Meguro, Tokyo 153-8902, Japan

Supporting Information

ABSTRACT: Copper oxide clusters, $Cu_nO_m^+$, were prepared in the gas phase by laser ablation of a copper rod in the presence of oxygen. The cluster ions were heated up to 1000 K downstream from the cluster source (post heating), and the abundance of $Cu_nO_m^+$ (n = 4−19) was examined using mass spectrometry. Temperature-programmed desorption experiments revealed that an oxygen molecule is released from oxygen-rich $Cu_nO_{m+\delta}^+$ ($m \approx n/2 + 1$; δ = 1−4), forming near-stoichiometric $Cu_nO_{m+\delta}^+$ (δ = 0−1) below T = 500 K. Oxygen molecules are further released from cluster ions to form $Cu_nO_{m+\delta}^+$ (δ = −1, 0) above 800 K, suggesting that a Cu atom can take a +1 charge state at high temperatures. In relation to their thermal stability, we observed the reactivity of $Cu_nO_m^+$ with NO molecules. It was found that NO readily attaches to $Cu_nO_m^+$ cluster ions, forming $Cu_nO_mNO^+$ with pseudo-first-order rate constants of $\sim 10^{-10}$ cm^3 s^{-1}. The post heating of Cu_nO_m NO^+ to 523 K revealed that oxygen-rich $Cu_nO_m^+$ ($Cu_6O_5^+$, $Cu_8O_6^+$, $Cu_9O_7^+$, and $Cu_{11}O_8^+$) reacts with NO to form $Cu_nO_{m-1}^+$ and NO_2, as expressed by $Cu_nO_m^+ + NO \rightarrow Cu_nO_{m-1}^+ + NO_2$.

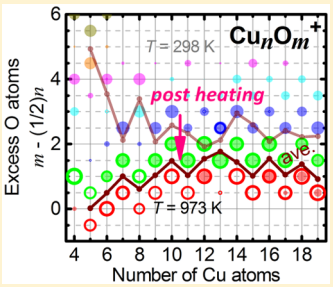

1. INTRODUCTION

Two stable compositions, CuO and Cu_2O (cupric and cuprous oxide, where Cu atoms take Cu(II) and Cu(I) oxidation states, respectively), are well-known stable copper oxides in the bulk phase. However, the nonstoichiometry of copper oxides, such as that which forms $Cu_2O_{1+\gamma}$, has been investigated by many researchers:[1−6] Wieder and Czanderna and other groups studied the oxidation of a copper thin film at low temperature, and found thermally stable $CuO_{0.67}$ (also Cu_3O_2 or $Cu_{1.5}O$).[1−4,7,8] Tretyakov et al. reported nonstoichiometry and defect structures in copper oxides and ferrites, found by high-temperature electrochemical measurements.[9] Their measurements correspond to defect models that allowed the calculation of the absolute magnitudes and the pressure dependencies of the defects in these compounds. They explained that the existence of $Cu_{1.5}O$ can be understood as a much larger oxygen deficit of $Cu_2O_{1+\gamma}$.

It is conceivable that different oxidation states of copper could provide different reactivities. For instance, Cu_2O is known to exhibit a higher activity for CO oxidation than CuO,[10] which originates from its ability to seize or release surface lattice oxygen more readily than CuO and Cu. Furthermore, the nonstoichiometric metastable copper oxide species formed during the reduction is very active for CO oxidation, because of its excellent ability to transport surface lattice oxygen. Here, we are confronted with the question of what excess of oxygen atoms is needed to be reactive toward small molecules in the gas phase.

Given this background, we focused our study on copper oxide clusters in the gas phase: gas phase clusters studied with mass spectrometry give good insight into stabilities and reactions at the atomic and molecular levels,[11,12] because sizes, stoichiometries, and oxidation states, which may determine reactivity, can be controlled at will. Gas-phase copper oxide clusters have been investigated by many researchers.[8,13−23] Gord and co-workers reported the stoichiometry of copper oxide cluster ions that were prepared by laser desorption/ionization from a pellet of copper oxide: Cu:O ratios of 1:0.5 and 1:0.6 were predominantly formed for the cations and anions, respectively.[13] They also elucidated the loss of fragments, including Cu and O atoms, from the clusters by collision-induced dissociation (CID) of the copper oxide cluster ions with argon. Aubriet et al. observed $Cu_nO_m^+$ (n = 1−10) and $Cu_nO_m^-$ (n = 1−13) formed by the laser ablation of a CuO sample.[19] They found a series of cluster ions, $(Cu_2O)_nCu^+$, $(Cu_2O)_nCu_2O^+$, $(Cu_2O)_nO_2^-$, and $(Cu_2O)_nCuO_2^-$. From a theoretical point of view, Jadraque and Martin reported stable structures of $(Cu_2O)_n^+$ and $[(Cu_2O)_nCu]^+$.[24] They concluded that the cluster-growing process proceeds by the aggregation of Cu_2O to $Cu_{n-2}O_{m-1}^+$, and involves bonding between the divalent O atom in the monomer unit and a single coordinated terminal Cu atom in the parent cluster. Wang et al. studied the electronic structure of small copper oxide clusters, from Cu_2O to Cu_2O_4, through photoelectron spectroscopy and density functional calculations.[25] They succeeded in reproducing the experimentally observed trend with computational results.[26]

Special Issue: Current Trends in Clusters and Nanoparticles Conference

Received: November 27, 2014
Revised: February 3, 2015

DOI: 10.1021/jp511840d
J. Phys. Chem. C XXXX, XXX, XXX−XXX

In a previous study, we prepared copper oxide cluster ions in the gas phase; these thermally stable compositions were investigated after placing the cluster ions in thermal equilibrium at 573 K (post heating).[27] It was found that $Cu_nO_m^{\pm}$ was selectively and abundantly observed at 573 K, with the ratio n:m originally described as approximately 3:2, $5 \leq n \leq 12$, although now we can describe this much better: $m \approx n/2 + \delta$, $\delta = 1-2$. From this stoichiometry, $Cu_nO_m^+$ is considered to be $(CuO)_x(Cu_2O)_y^+$, comprised of both Cu(I) and Cu(II), indicating that mixed valence states exist at 500 K. However, there were several issues that remained in question: Why was the observed cluster composition different from the bulk phase one? Is the stable stoichiometry dependent on temperature? How do oxygen-rich copper oxide clusters converge into the mixed valence states, $(CuO)_x(Cu_2O)_y^+$? How reactive are the mixed valence clusters? To answer these questions, we extended the cluster size range and also the temperature range. We carefully scanned the post heating temperature up to 1000 K, and obtained pseudo temperature-programmed desorption (TPD) plots for the copper oxide clusters in the present study. The TPD technique has been applied to the study of gas phase metal oxide clusters by Lang and co-workers at low temperature (80−300 K).[28,29] In the present study, we investigated the desorption of oxygen molecules at higher temperatures (300−1000 K). In addition, we studied the reactivity of these clusters with NO in the gas phase in relation to thermally stable stoichiometry.

2. EXPERIMENTAL SECTION

The stable stoichiometry and reactivity of copper oxide cluster ions was investigated using a reflectron-equipped time-of-flight (TOF) mass spectrometer.[27,30−32] Copper oxide clusters were prepared in the presence of oxygen gas diluted in helium (total stagnation pressure 0.9 MPa; purities of >99.99995% (He) and 99.9% (O_2); pulse duration ~400 μs) by laser ablation of a cluster source: a copper metal rod (Nilaco Co., Ltd., 99.99%) was vaporized using the second harmonic of a Nd:YAG laser (532 nm) at a typical pulse energy of 10 mJ. Oxygen diluted in helium was supplied to the cluster source from a pulsed valve. After the clusters were thus prepared, they were passed through a reaction gas tube (2 mm diameter, 60 mm length) and then introduced into an extension tube (4 mm diameter, 120 mm length), where they were heated (post heating). The temperature of the extension tube was controlled in the range of 300−1000 K using a resistive heater, and monitored using a thermocouple (type K).[32] The residence time of the cluster ions and the number density of the He gas in the extension tube were estimated to be longer than 100 μs and greater than 10^{18} cm^{-3}, respectively. Hence, a thermal equilibrium of the clusters was achieved by collisions with the He carrier gas well before expansion into the vacuum. Pseudo-TPD plots were obtained by scanning over the temperature range gradually.

When a reaction of the cluster ions with NO was observed, the reactant NO gas, which was injected into the reaction gas tube using a pulsed valve, was diluted by He so that the total pressure was constant at 0.1 MPa (pulse duration ~500 μs). The typical number density of the reactant gas inside the reaction tube was estimated to be 10^{16} cm^{-3}. The residence time of the copper oxide cluster ions in the reaction gas tube was estimated to be around 70 μs. To summarize, our experimental setup was such that the reaction of the copper oxide clusters with NO occurred in the reaction tube, which was maintained at room temperature, and then the clusters were passed through the extension tube controlled at a determined temperature (post heating).

The cluster ions gained a kinetic energy of 3.5 keV in the acceleration region for the mass analysis. The ions were steered and focused by a set of vertical and horizontal deflectors and an einzel lens. After traveling through a 1 m field-free region, the ions were reversed by the reflectron and detected with a double-microchannel plate detector (Hamamatsu Photonics). Signals from the detector were amplified with a 350 MHz preamplifier (Stanford Research Systems SR445A) and digitized using an oscilloscope (LeCroy LT374). Averaged TOF spectra (typically averaged over 500 sweeps) were sent to a computer for analysis. The mass resolution, $m/\Delta m$, exceeded 1000. The intensity of the mass peaks were evaluated by deconvolution using isotope patterns for $Cu_nO_m^+$, $Cu_nO_m(H_2O)^+$, and $Cu_nO_m(H_2O)_2^+$ (see Supporting Information).

3. RESULTS AND DISCUSSION

3.1. Release of Oxygen Molecule by Post Heating.

Figure 1a shows a mass spectrum of copper oxide cluster cations produced by laser ablation of a copper metal rod in the presence of 0.5% oxygen gas in helium without postheating

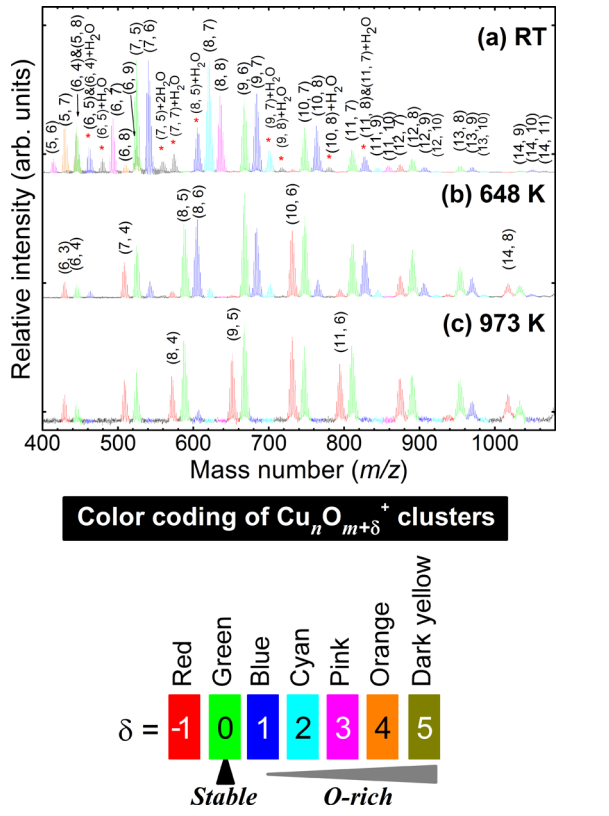

Figure 1. (a) Mass spectrum of $Cu_nO_m^+$ produced by laser ablation of a copper metal rod in the presence of 0.5% oxygen gas in He. Numbers in parentheses indicate the n and m values of $Cu_nO_m^+$. Asterisks (*) stand for water adducts. The oxygen number is color coded from the smaller side in the following order: red, green, blue, cyan, pink, orange, and dark yellow. Green corresponds to thermally stable compositions, such as $Cu_{12}O_8^+$ and $Cu_{15}O_9^+$. (b) Mass spectrum of $Cu_nO_m^+$ after post heating in the extension tube, controlled at 648 K. (c) Mass spectrum of $Cu_nO_m^+$ after post heating in the extension tube, controlled at 973 K. The intensities of the measurements in panels a, b, and c are scaled 1, 4, and 24 times, respectively.

DOI: 10.1021/jp511840d
J. Phys. Chem. C XXXX, XXX, XXX−XXX

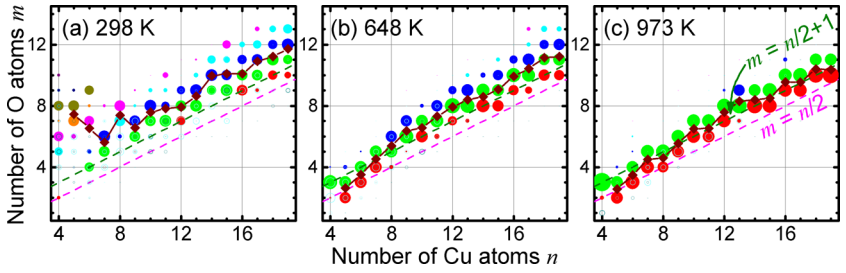

Figure 2. Relative abundances of $Cu_nO_m^+$ (n = 4−19) for different numbers of Cu and O atoms at (a) room temperature, (b) 648 K, and (c) 973 K. Bubble size represents the relative abundance normalized in each column of n. Colors are selected in the same way as in Figure 1. Contribution from water adducts, $Cu_nO_m(H_2O)^+$ and $Cu_nO_m(H_2O)_2^+$, are depicted as unfilled gray circles.

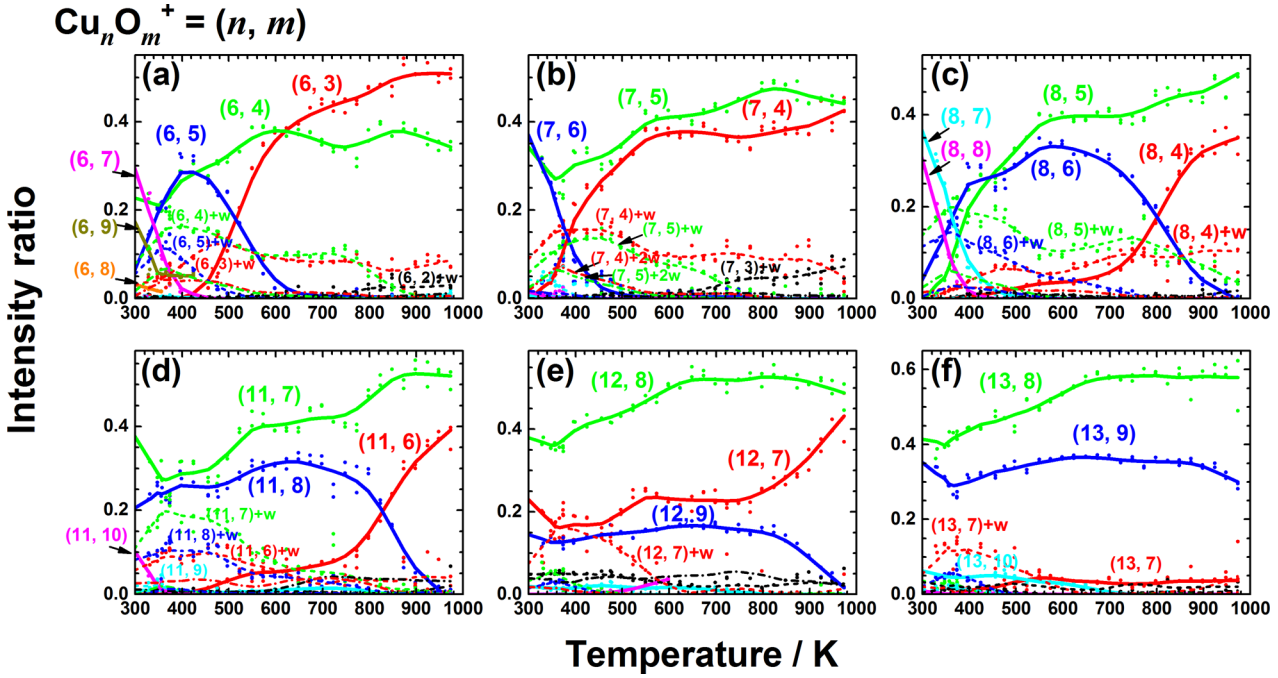

Figure 3. TPD profiles of $Cu_nO_m^+$ (n = 6−8, 11−13), exhibiting the intensity ratios of each cluster ion as a function of the temperature of the extension tube. The rate of heating of the extension tube was 1.4 K min^{-1}. Solid lines were drawn by smoothing the recorded data points, as eye guides. Numbers in parentheses indicate the (n, m) values of $Cu_nO_m^+$. The intensity of $Cu_nO_m^+$ was normalized such that sum of intensities, $\Sigma_m Cu_nO_m(H_2O)_{0-2}^+$, equals one for each n. The oxygen number is color coded in the same way as in Figure 1. The dashed and dashed-dot lines indicate the intensities of $Cu_nO_m(H_2O)^+$ and $Cu_nO_m(H_2O)_2^+$ clusters (denoted as (n, m) + w and (n, m) + 2w, respectively).

treatment. Peaks assignable to $Cu_nO_{m+\delta}^+$ (for most cases $m \approx n/2 + 1$; δ = ∼1) appeared in the mass spectrum, where δ denotes the number of excess oxygen atoms from the thermally stable composition $Cu_nO_m^+$ shown below. Here, the clusters, $Cu_nO_m^+$, are color-coded according to the following rules: thermally stable compositions such as $Cu_7O_5^+$ and $Cu_{12}O_8^+$ are labeled in green, and clusters emerging after the post heating such as $Cu_7O_4^+$ and $Cu_{12}O_7^+$ are in red. Then, the clusters are color-coded in the order of the number of oxygen atoms, with red, green, blue, cyan, pink, orange, dark yellow, and dark blue corresponding to δ = −1, 0, 1, 2, 3, 4, 5, and 6 (see Supporting Information Figure S2 for details). Some water adducts, for example, $Cu_7O_5(H_2O)_2^+$, $Cu_8O_5(H_2O)^+$, and $Cu_{11}O_7(H_2O)^+$ were also produced. Details on their origins and temperature dependences are discussed in the Supporting Information. In order to visualize the changes in cluster stoichiometry with temperature, bubble plots of the relative abundances of $Cu_nO_m^+$ (n = 4−19) are shown in Figure 2. Since no significant fragmentation paths involving a change in the number of metal atoms were found, cluster abundance was normalized in each column of n. In most cases, the distribution of abundantly formed clusters lies in the band of $m \approx n/2 + 1+\delta$, with δ = 1, 2, and 3 (blue, cyan, and pink). Therefore, the trend can be described in terms of average oxygen numbers (AONs), drawn as a line plot in Figure 2. At room temperature, the AONs are roughly given by $m \approx n/2 + 2$ (the overlap with the clusters marked in blue; δ = 1). For the small sized clusters of $n \leq 8$, oxygen ultrarich clusters ($\delta \geq 4$) such as $Cu_4O_{6,8}^+$, $Cu_5O_{7,8}^+$, $Cu_6O_{7,9}^+$, and $Cu_8O_{7,8}^+$ are abundantly formed.

Figure 1b shows the mass spectrum of $Cu_nO_m^+$ clusters after they were heated in the extension tube at 648 K. Abundances of oxygen-rich $Cu_nO_m^+$ clusters (indicated in blue, cyan, and pink; δ = 1, 2, and 3), such as $Cu_6O_7^+$, $Cu_8O_7^+$, $Cu_8O_8^+$, $Cu_{10}O_8^+$, and $Cu_{11}O_{10}^+$, were reduced compared with what was observed in the room temperature spectra. In contrast, abundances of more oxygen-poor $Cu_nO_m^+$ species (red and green; δ = −1, 0) such as $Cu_6O_{3,4}^+$, $Cu_7O_4^+$, $Cu_8O_{5,6}^+$, $Cu_{10}O_6^+$ and $Cu_{11}O_6^+$ increased, or in some cases newly appeared. Oxygen ultrarich clusters ($\delta \geq 4$) that were observed at room temperature disappeared; hence, these copper oxide clusters are considered

DOI: 10.1021/jp511840d
J. Phys. Chem. C XXXX, XXX, XXX−XXX

to bind oxygen molecules weakly. As a result, the stoichiometries of the clusters shifted to the line of $m \approx n/2 + 1$, as shown in Figure 2b, except for those of small-sized clusters ($n \leq 8$). For the small-sized clusters, a drastic change in AON occurs so that the AON lies on the line of $m \approx n/2 + 1$. By elevating the temperature to 973 K (see Figure 1c), $Cu_nO_m^+$ clusters that included lower numbers of oxygen atoms (red; $\delta = -1$) such as $Cu_8O_4^+$, $Cu_9O_5^+$, and $Cu_{11}O_6^+$ began to appear. By contrast, the oxygen-rich clusters (blue; $\delta = 1$) such as $Cu_8O_6^+$, $Cu_9O_7^+$, and $Cu_{11}O_8^+$ decreased. Therefore, the line of AONs overlapped with the line of $m \approx n/2 + 1$. It is worth noting that the remaining clusters had two adjacent oxygen numbers for each n (green and red), except for $n = 4$ and 13.

The mechanism of the dissociation of the clusters by heat was investigated by a pseudo-TPD experiment, in which we measured the abundances of $Cu_nO_m^+$ as a function of the temperature of the extension tube. In a *conventional* TPD experiment for a solid surface, species dissociating from the solid sample are observed by mass spectrometry as the temperature of the sample is gradually raised at a constant speed. By contrast, a bunch of pristine cluster ions was supplied from the cluster source at the rate of 10 Hz in the *gas phase* TPD experiment. Hence, we were able to obtain temperature dependences as the temperature either increased or decreased. In fact, we observed temperature dependences in both rise and fall modes, and confirmed that they were essentially the same as long as the speed of the temperature change was slow enough. Figure 3 shows the pseudo-TPD data for $Cu_nO_m^+$ ($n = 6-8$ and 11−13). Again, the same color code is used to distinguish the different oxygen numbers in the clusters. Here, the intensity of $Cu_nO_m^+$ has been normalized such that the sum of the intensities ($\Sigma_m Cu_nO_m(H_2O)_{0-2}^+$) equals 1 for each n. Note that ion signals decreased with an increase in the temperature regardless of ion size, probably because each ion cluster expanded thermally in the molecular beam, lowering the detection efficiency of the TOF mass spectrometer. For $n = 7$, the intensity of $Cu_7O_6^+$ decreases at 400 K, whereas the relative intensity of $Cu_7O_4^+$ increases at the identical temperature. By contrast, the relative intensity of $Cu_7O_5^+$ (or more precisely, the sum of the intensities of $Cu_7O_5^+$ and its water adduct, $Cu_7O_5(H_2O)^+$) remains constant. These findings indicate that an oxygen molecule is released from $Cu_7O_6^+$, as

$$Cu_7O_6^+ \xrightarrow{\Delta} Cu_7O_4^+ + O_2 \quad (1)$$

For $n = 8$, the relative intensity of $Cu_8O_8^+$ gradually decreases and approaches zero at 400 K. In accordance with this decay, the relative intensity of $Cu_8O_6^+$ increases as the temperature is raised from 300 K, and reaches ∼0.3 at 450 K. Then, it begins to decrease above 600 K, and $Cu_8O_4^+$ starts to increase in the same temperature range. These intensity changes indicate a sequential oxygen release from $Cu_8O_8^+$, as

$$Cu_8O_8^+ \xrightarrow{\Delta} Cu_8O_6^+ + O_2 \xrightarrow{\Delta} Cu_8O_4^+ + 2O_2 \quad (2)$$

In addition, it is seen that $Cu_8O_7^+$ decreases and approaches zero in the range of 400−500 K, while $Cu_8O_5^+$ increases by the same extent in the same temperature range, indicating oxygen release from $Cu_8O_7^+$, as

$$Cu_8O_7^+ \xrightarrow{\Delta} Cu_8O_5^+ + O_2 \quad (3)$$

The other clusters also behave in a similar fashion, as summarized in Figure S3. Namely, the clusters, defined as $Cu_nO_m^+$ (green; $\delta = 0$), remain unchanged, and an oxygen-rich $Cu_nO_{m+1}^+$ cluster (blue; $\delta = 1$) releases an oxygen molecule to give a $Cu_nO_{m-1}^+$ cluster (red; $\delta = -1$):

$$Cu_nO_{m+1}^+ \xrightarrow{\Delta} Cu_nO_{m-1}^+ + O_2 \quad \text{(blue} \rightarrow \text{red)} \quad (4)$$

$$Cu_nO_m^+ \xrightarrow{\Delta} \text{(no reaction up to1000 K)}$$
$$\text{(green; no change)} \quad (5)$$

These concomitant changes, which appear for all n studied, indicate an oxygen molecule release from $Cu_nO_m^+$. Hence, we are able to conclude that the oxygen molecule release from $Cu_nO_m^+$ is the main dissociation pathway at high temperatures. Since the intensities of $Cu_nO_m^+$ have been normalized within each same number of copper atoms, n, the pairwise changes could misrepresent oxygen molecule release if there existed only two cluster ions having a different m at the same n: the decrease of one ion would increase the relative intensity of the other ion, even if its intensity is actually unchanged. However, in the present study, more than three ions having different m values were involved. Hence, the concomitant changes in each n make evident the fact of oxygen molecule release from the clusters. As far as we observed, all the changes were explained in terms of oxygen and water molecule releases. No clear signs were observed to indicate a release of a copper metal atom.

It is well known that an oxygen atom takes a −2 oxidation state, and that copper atoms commonly adopt Cu(I) and Cu(II) as their oxidation states. These oxidation states coexist in an oxide cluster ion, with copper atoms in the oxides preferring the Cu(I) state at higher temperatures.[33] Let us consider the charge balance in a copper oxide cluster. $Cu_nO_m^+$ can be expressed by a combination of CuO and Cu_2O units, excess oxygen atoms, and metallic Cu(0) atoms. For instance, $Cu_{10}O_8^+$ could be described as $(CuO)_6(Cu_2O)_2^+$ or $(CuO)_2(Cu_2O)_4(O_2)_1^+$, whereas $Cu_6O_7^+$ could be described as $(CuO)_4(Cu_2O)_1(O_2)_1^+$, and $Cu_5O_2^+$ as $(Cu_2O)_2(Cu)_1^+$. Hence, the release of oxygen would correspond to an increase of Cu_2O units and a decrease of CuO units in the clusters, as

$$Cu_{10}O_8^+ \xrightarrow{\Delta} Cu_{10}O_6^+ + O_2 \quad (6)$$

$$(CuO)_6(Cu_2O)_2^+ \xrightarrow{\Delta} (CuO)_2(Cu_2O)_4^+ + O_2 \quad (7)$$

Here, four (CuO) units change into two Cu_2O units upon the release of an O_2 molecule. Other clusters can be written in units in a similar way; the expected numbers of units in $Cu_nO_m^+$ clusters are summarized as a map in Figure S4.

It should be noted that the determination of the numbers of units is not unique. However, considering that the O_2 release occurs at a relatively low temperature (a 50% intensity increase for $Cu_{10}O_8^+$ occurs at 400 K), it seems that the notation of $(CuO)_2(Cu_2O)_4(O_2)_1^+$ is suitable:

$$(CuO)_2(Cu_2O)_4(O_2)_1^+ \xrightarrow{\Delta} (CuO)_2(Cu_2O)_4^+ + O_2 \quad (8)$$

This notation is also applicable for the other example:

$$Cu_{11}O_8^+ \xrightarrow{\Delta} Cu_{11}O_6^+ + O_2 \quad (9)$$

$$(CuO)_5(Cu_2O)_3^+ \xrightarrow{\Delta} (CuO)_1(Cu_2O)_5^+ + O_2 \quad (10)$$

$$(CuO)_1(Cu_2O)_5(O_2)_1^+ \xrightarrow{\Delta} (CuO)_1(Cu_2O)_5^+ + O_2 \quad (11)$$

DOI: 10.1021/jp511840d
J. Phys. Chem. C XXXX, XXX, XXX−XXX

To summarize the TPD results of the observed clusters, the overall trend of the temperature ranges of the oxygen release was plotted as a bar graph in Figure S6. In the low temperature range (T < 400 K), excess oxygen atoms (dark yellow, orange, pink, and cyan; $\delta \geq 2$) are released to a greater extent with increasing temperature. Then in the range of 400 K < T < 650 K, some oxygen-rich clusters (blue; $\delta = 1$) release an oxygen molecule and produce near-stoichiometric clusters (red; $\delta = -1$). One of the near-stoichiometric $Cu_nO_m^+$ clusters (green; $\delta = 0$) remains unchanged during the post heating (up to 1000 K). In the much higher temperature range of 700 K < T < 850 K, the rest of the oxygen-rich clusters start to emit oxygen molecules. Finally, in the range of 850 K < T < 1000 K, the only remaining clusters are $Cu_nO_m^+$ (red and green; $\delta = -1,0$).

3.2. Reaction with NO. As copper atoms can exist in both Cu(I) and Cu(II) states, copper oxide clusters are expected to transfer oxygen atoms to small molecules, such as NO. Given this relation, the reactivity of $Cu_nO_m^+$ with NO was investigated at room temperature. Figure 4 shows mass spectra of copper

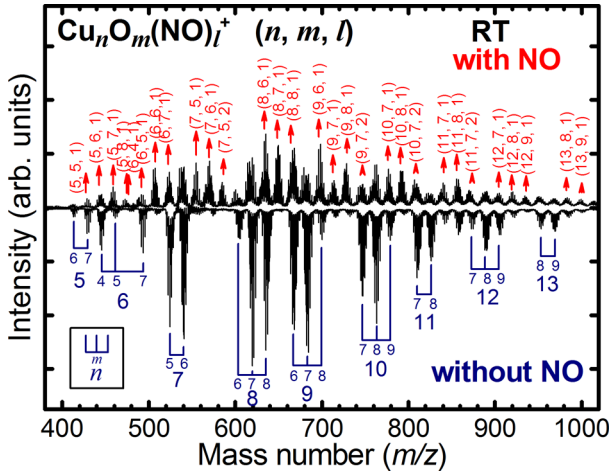

Figure 4. Mass spectra of ions produced after $Cu_nO_m^+$ clusters passed through the reaction gas tube, with and without 0.35% NO diluted in He gas, at room temperature (RT). $Cu_nO_m^+$ clusters were produced by laser ablation of a copper metal rod in the presence of 0.5% oxygen gas in a helium carrier gas. NO adducts that were formed after the reaction are indicated by red arrows.

oxide cluster cations after they passed through the reaction tube filled with 0.35% NO reactant gas. The intensity of $Cu_nO_m^+$ clusters was found to decrease, but their single or double NO adducts $Cu_nO_m(NO)_{1,2}^+$ appeared after the reaction, indicating that NO simply attached to $Cu_nO_m^+$, as

$$Cu_nO_m^+ + NO \rightarrow Cu_nO_mNO^+ \quad (12)$$

At higher NO gas concentrations, multiple NO adducts, $Cu_nO_m(NO)_{2-3}^+$, were also observed. The pseudo-first-order rate constants of this attachment reaction were measured by changing the concentration of NO (0.04–0.1%) while keeping the total gas pressure constant. The rate constants for $Ni_nO_m^+$ with NO have been reported by Vann et al., and the reaction rate of $Ni_7O_8^+$ is known to be 5.6×10^{-10} cm^3 s^{-1}.[34] Therefore, the rate constants for $Cu_nO_m^+$ with NO were calibrated by measuring the reaction rate constant of $Ni_7O_8^+$ with NO during the same experiment. As shown in Figure 5, the rate constants k_{ad} (representing the rate of adsorption) ranged from 10^{-9} to 10^{-10} cm^3 s^{-1} for all the cluster ions studied. According to the

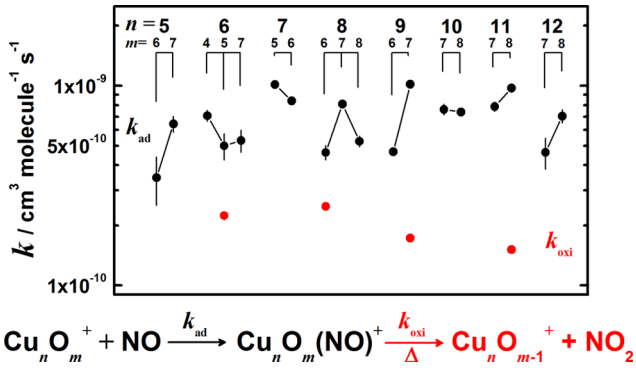

Figure 5. Pseudo-first-order rate constants k_{ad} (for the adsorption reaction, $Cu_nO_m^+ + NO \rightarrow Cu_nO_mNO^+$) and k_{oxi} (for the NO oxidation reaction, $Cu_nO_m^+ + NO \rightarrow Cu_nO_{m-1}^+ + NO_2$), as a function of the composition (n, m) of $Cu_nO_m^+$ clusters.

Langevin cross section, which gives an uppermost cross section relating to charge-induced dipole interactions, the cross sections with NO and the rate constant are estimated to be 1.4×10^{-18} m^2 and 2.3×10^{-9} cm^3 s^{-1}, respectively. A comparison of the rate constants suggests that NO is able to attach to the copper oxide clusters at almost every collision.

It is difficult to know, using only simple mass spectrometry, how NO binds to $Cu_nO_m^+$ clusters. Hence, we observed the reaction products after post heating. Figure 6 shows the mass

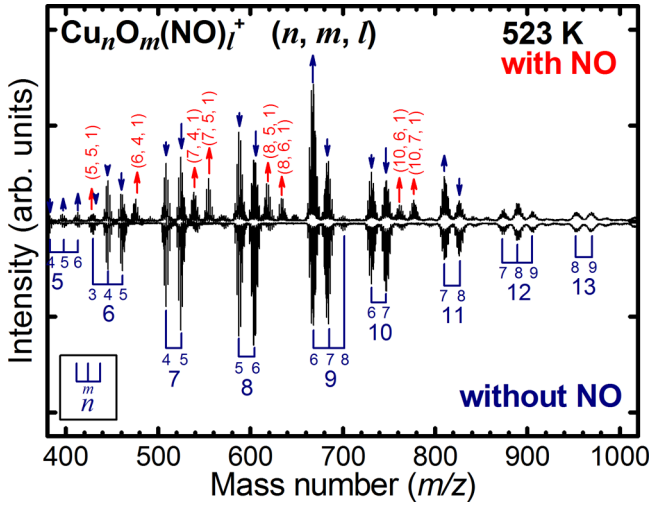

Figure 6. Mass spectra of ions produced after $Cu_nO_m^+$ clusters passed through the reaction gas tube, with and without 0.7% NO diluted in He gas, with the extension tube heated to 523 K. Clusters whose intensities increased and decreased with the addition of NO in the gas tube are indicated by arrows.

spectra of the copper oxide cluster cations both after the reaction with 0.7% NO gas and without the NO reaction, followed by post heating treatment at 523 K. It should be noted that the reaction tube where the clusters react with NO gas was kept at room temperature. Namely, the reaction products were formed whether or not the extension tube downstream was heated. It was seen that $Cu_5O_5NO^+$, $Cu_6O_4NO^+$, $Cu_7O_4NO^+$, $Cu_7O_5NO^+$, $Cu_8O_5NO^+$, $Cu_8O_6NO^+$, $Cu_{10}O_6NO^+$, and $Cu_{10}O_7NO^+$ still remained in the mass spectra even after the post heating, suggesting that the binding energies between NO and those clusters were sufficiently high compared to those of the other NO adducts. In contrast, the $Cu_9O_7NO^+$ that had

DOI: 10.1021/jp511840d
J. Phys. Chem. C XXXX, XXX, XXX−XXX

been formed by the reaction between $Cu_9O_7^+$ and NO at room temperature disappeared after the post heating (see Figures 4 and 6). In addition, comparing the upper and the lower mass spectra in Figure 6, one finds that the intensity of $Cu_9O_7^+$ decreases, and the intensity of $Cu_9O_6^+$ increases to a similar extent. Figure 7 shows the ratios of the intensities of clusters

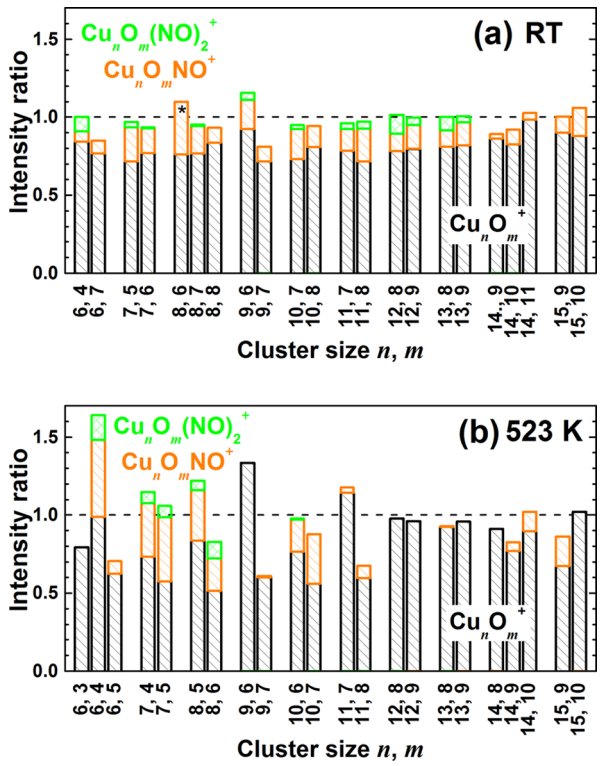

Figure 7. Ratios of the intensities of the NO reaction products $Cu_nO_m^+$ and $Cu_nO_mNO^+$ to those of pristine $Cu_nO_m^+$ (not exposed to NO), without and with post heating to 523 K, using 0.35% and 0.7% NO diluted in He gas, respectively. Data are taken from the same spectra shown in Figures 4 and 6.

that have reacted with NO (both $Cu_nO_m^+$ and $Cu_nO_mNO^+$) to those of pristine $Cu_nO_m^+$ that has not been exposed to NO, as observed after the post heating treatment—in essence, the ratios of $Cu_nO_m^+$ after the reaction range from 0.5 to 1.0, and those of $Cu_nO_mNO^+$, from 0.1 to 0.5. For $Cu_6O_3^+$, $Cu_7O_4^+$, $Cu_7O_5^+$, $Cu_{10}O_6^+$, $Cu_{10}O_7^+$, $Cu_{12}O_8^+$, and $Cu_{12}O_9^+$, the sum of the intensity ratios of $Cu_nO_m^+$ and $Cu_nO_mNO^+$ equals almost 1, suggesting that during the reaction, NO simply attaches to $Cu_nO_m^+$.

By contrast, there are some cluster ions for which the summation of the intensity ratios deviates significantly from 1. Examining the summations for clusters at 523 K closely, there are several pairs of $Cu_nO_m^+$ and $Cu_nO_{m-1}^+$ clusters whose summation after the reaction with NO increases and decreases from 1 to a similar extent: $Cu_6O_5^+$ and $Cu_6O_4^+$, $Cu_8O_6^+$ and $Cu_8O_5^+$, $Cu_9O_7^+$ and $Cu_9O_6^+$, and $Cu_{11}O_8^+$ and $Cu_{11}O_7^+$. This finding indicates that NO extracts an oxygen atom from $Cu_nO_m^+$, as in eq 13:

$$Cu_nO_m^+ + NO \rightarrow [Cu_nO_m^+NO] \rightarrow [Cu_nO_{m-1}^+NO_2] \xrightarrow{\Delta} Cu_nO_{m-1}^+ + NO_2 \quad (13)$$

By analyzing the concentration dependence of intensity changes of parent clusters, the rate constants k_{oxi} (representing the rate of oxidation) for clusters with (m, n) values of (6, 5), (8, 6), (9, 7), and (11, 8) were found to range from 1 to 2 × 10^{-10} cm^3 s^{-1}, as shown in Figures 5 and S7. This is 1 order smaller than the rate constant for NO addition, k_{ad}. It implies that the oxidation reaction proceeds when the NO adducts ($Cu_nO_m^+NO$) gain energy by post heating, and the smaller value of the rate constant k_{oxi} reflects the branching ratio between the dissociation of NO and the O atom transfer to NO. According to the result of a temperature-programmed reduction (TPR) experiment on bulk CuO_x with hydrogen gas as reported by Ferrandon et al., the TPR peak lies at 480 K.[35] Although the reduction of copper oxide seems to proceed more easily in the presence of hydrogen gas compared with an oxygen-doped helium carrier gas, the temperature range (400 K < T < 650 K) of the oxygen release from oxygen-rich clusters (blue) implies that their oxygen is ready to use in a chemical reaction.

The reaction of $Cu_nO_m^+$ (n = 3–19, $m \leq 9$) with NO has been studied by Hirabayashi and Ichihashi under single-collision conditions using collision-induced dissociation for size-selected cluster ions.[36] They observed three reaction channels: NO adsorption, O_2 release, and O release. All of these reaction channels were also observed in the present study, where all the reactions are considered to occur under thermal conditions. The oxidation of (8, 6) was not mentioned in their paper. For NO adsorption, they found that the reaction cross sections were smaller than 2 × 10^{-20} m^2 at a collision energy of 0.2 eV (with a typical spread of 0.4 eV in the full width at half-maximum). This difference in the cross sections may originate from the collision energy in a CID experiment and available energy generated in the clusters upon adsorption of NO. In our experiment, the reactions occur with thermal energy (at room temperature), and the energy generated upon the adsorption of NO is readily removed from the clusters by their frequent collisions with He atoms in the reaction tube (>10^3 collisions). Note that the ratio of NO to He is ≪1%, since the carrier gas dilutes the injected reactant gas. In fact, we observed a dissociation of NO from the $Cu_nO_mNO^+$ clusters when they were heated in the extension tube. These findings suggest that, for the single-collision condition, NO that had temporarily adsorbed onto $Cu_nO_m^+$ dissociated from it with the available energy, lowering the nominal reaction cross section. For O_2 release, Hirabayashi and Ichihashi found that the reaction cross section increased with an increase in the collision energy, suggesting that there is a barrier for the formation of $Cu_nO_{m-2}^+$ and/or that the reaction is endothermic. This result is totally consistent with ours, showing that oxygen molecules are released from the cluster ions at higher temperatures. For O_2 release (as given by eq 6), since the formation cross section of $Cu_nO_{m-1}^+$ and the reaction with NO decreases with increased collision energy in the CID experiment, the reactions are suggested to proceed exothermically. Hence, the NO_2 formation reaction itself is considered to proceed at room temperature, and post heating was needed in our experiment to remove NO_2 from $Cu_nO_{m-1}^+$.

In our previous study, we examined the reactivity of $Cu_nO_m^+$ with CO, which binds very weakly to $Cu_9O_6^+$ and $Cu_{12}O_8^+$, whose stoichiometry can be written as $(CuO)_k(Cu_2O)_k^+$ (k = 3, 4). For the reactions studied here, NO was found to bind to $Cu_9O_6^+$ and $Cu_{12}O_8^+$, but mostly dissociated from these species when heated to 523 K. This finding suggests that the interaction of $(CuO)_k(Cu_2O)_k^+$ (k = 3, 4) with NO is also very weak. In fact, Sugawara el al. reported the reactivity of

DOI: 10.1021/jp511840d
J. Phys. Chem. C XXXX, XXX, XXX–XXX

$Cu_nO_m^+$ with NO via Fourier transform ion cyclotron resonance (FT-ICR) mass spectrometry, where they observed the formation of $Cu_nO_mNO^+$ clusters and their subsequent reactions while increasing the collision numbers up to 60 collisions.[22] According to their results, $Cu_{12}O_8^+$ and $Cu_{13}O_8^+$ clusters are exceptionally inert, while other clusters were oxidized or reduced by reactions with NO.

$$Cu_nO_m(NO)_l^+ \rightarrow Cu_nO_m(NO)_{l-2}^+ + N_2 \quad (n = 5-11) \tag{14}$$

$$Cu_nO_m(NO)_l^+ \rightarrow Cu_nO_{m-1}(NO)_{l-1}^+ + NO_2 \quad (n = 2-4, 12-15) \tag{15}$$

In this analogy, the cluster ions that actually oxidize NO can be expressed as clusters with a single oxygen atom excess, such as $(CuO)_k(Cu_2O)_kO^+$ and $(CuO)_k(Cu_2O)_{k+1}O^+$ (k = 2, 3). It is likely that the excess oxygen atom participates in the NO oxidation reaction, forming $(CuO)_k(Cu_2O)_k^+$ and $(CuO)_k(Cu_2O)_{k+1}^+$ (k = 2, 3). Our pseudo-TPD experiments indicated that these product species are thermally stable in the whole temperature range studied.

It should be noted that $(CuO)_k(Cu_2O)_kO^+$ and $(CuO)_k(Cu_2O)_{k+1}O^+$ (k = 2, 3), which are able to oxidize NO, exhibit similar temperature dependencies in the TPD plots shown in Figures 3 and S1: $Cu_8O_6^+$, $Cu_9O_7^+$, and $Cu_{11}O_8^+$ each release an oxygen molecule around 800 K, and $Cu_6O_5^+$ does so at 500 K. Considering the fact that $Cu_nO_m^+$ clusters with $n \leq 6$ behave differently from those with $n \geq 7$, there is a strong correlation between their reactivity with NO and the release of oxygen. In fact, other clusters that do not release oxygen molecules do not transfer an O atom to NO. As the TPD profiles of $Cu_{17}O_{11}^+$ and $Cu_{19}O_{12}^+$ closely resemble those of $Cu_8O_6^+$ and $Cu_9O_7^+$, as can be seen in Figure S1, it is highly probable that $Cu_{17}O_{11}^+$ and $Cu_{19}O_{12}^+$ react with NO molecules (as $(CuO)_5(Cu_2O)_6^+$ and $(CuO)_5(Cu_2O)_7^+$, or specifically, $(CuO)_3(Cu_2O)_7O^+$ and $(CuO)_3(Cu_2O)_8O^+$; see Figure S3). However, the NO reactivity of $Cu_{19}O_{12}^+$ is difficult to estimate due to poor abundance, while $Cu_{17}O_{11}^+$ seems to be decreased and $Cu_{17}O_{10}^+$ increased by the reaction with NO.

CONCLUSION

Isolated copper oxide clusters, $Cu_nO_m^+$ (n = 4–19) were formed in the gas phase. Thermal dissociation and reactions of the cluster ions with NO were investigated using a post heating device. First, gas phase pseudo-TPD experiments revealed that water molecules and oxygen molecules are released from $Cu_nO_m^+$ clusters ($m \approx n/2 + 1 + \delta$; δ = 1–3) below T = 500 K. Further, oxygen molecules are released from the clusters above 800 K to form $Cu_nO_{m+\delta}^+$ ($m \approx n/2 + 1$; δ = −1–0), suggesting that Cu atoms tend to take the +1 charge state at T > 800 K. Second, we observed the reactivity of $Cu_nO_m^+$ with NO molecules. It was found that NO readily attaches to all the $Cu_nO_m^+$ cluster ions, forming $Cu_nO_mNO^+$ with pseudo-first-order rate constants of $\sim 10^{-10}$ cm^3 s^{-1}. The post heating of $Cu_nO_mNO^+$ at 523 K reveals that oxygen-rich $(CuO)_k(Cu_2O)_kO^+$ and $(CuO)_k(Cu_2O)_{k+1}O^+$ (k = 2, 3) clusters react with NO to form $Cu_nO_{m-1}^+$ and NO_2, expressed as $Cu_nO_m^+ + NO \rightarrow Cu_nO_{m-1}^+ + NO_2$. It is likely that clusters that are active for the NO oxidation reaction have single excess oxygen atoms from the stable ones, and also desorb O_2 around 800 K.

ASSOCIATED CONTENT

Supporting Information

Analysis of water adducts. TPD profiles of $Cu_nO_m^+$ (n = 4–19), categorized by the shape of blue colored oxygen-rich clusters (Figure S1). TPD profiles of the summation of nonhydrated $Cu_nO_m^+$ (n = 4–19) (Figure S2). Color coding of observed $Cu_nO_m^+$ (n = 4–19) and approximated abundances (Figure S3). Three groups of TPD profiles of $Cu_nO_{m-1}^+$, $Cu_nO_m^+$, and $Cu_nO_{m+1}^+$ (n = 4–19) (Figure S4). A map of the expected numbers of the CuO and Cu_2O units comprising $Cu_nO_m^+$ clusters (Figure S5). The evolution of abundantly observed copper oxide cluster cations with post heating (Figure S6). A semilogarithmic plot of the reaction kinetics for $Cu_9O_7^+$ and $Cu_{11}O_8^+$ clusters with NO, at room temperature and 523 K (Figure S7). This material is available free of charge via the Internet at http://pubs.acs.org.

AUTHOR INFORMATION

Corresponding Author

*E-mail: mafune@cluster.c.u-tokyo.ac.jp. Telephone: +81-3-5454-6597.

Notes

The authors declare no competing financial interest.

ACKNOWLEDGMENTS

This work was supported by a Grant-in-Aid for Scientific Research (A) (No. 25248004) and a Grant-in-Aid for Scientific Research (C) (No. 24550010) from the Ministry of Education, Culture, Sports, Science and Technology, Japan (MEXT) and by the Genesis Research Institute, Inc. for the cluster research.

REFERENCES

(1) Wieder, H.; Czanderna, A. The Oxidation of Copper Films to $CuO_{0.67}$. *J. Phys. Chem.* **1962**, *66*, 816–821.
(2) Clarke, E., Jr.; Czanderna, A. Optical Transmittance and Microgravimetric Studies of the Oxidation of ⟨100⟩ Single Crystal Films of Copper. *Surf. Sci.* **1975**, *49*, 529–536.
(3) Yanase, A.; Matsui, H.; Tanaka, K.; Komiyama, H. Optical Observation of Oxidation and Reduction of Small Supported Copper Particles. *Surf. Sci. Lett.* **1989**, *219*, L601–L606.
(4) Yanase, A.; Komiyama, H. In Situ Observation of Oxidation and Reduction of Small Supported Copper Particles Using Optical Absorption and X-ray Diffraction. *Surf. Sci.* **1991**, *248*, 11–19.
(5) Lenglet, M.; Kartouni, K.; Machefert, J.; Claude, J. M.; Steinmetz, P.; Beauprez, E.; Heinrich, J.; Celati, N. Low Temperature Oxidation of Copper: The Formation of CuO. *Mater. Res. Bull.* **1995**, *30*, 393–403.
(6) Mencer, D. E.; Hossain, M. A.; Schennach, R.; Grady, T.; McWhinney, H.; Gomes, J. A. G.; Kesmez, M.; Parga, J. R.; Barr, T. L.; Cocke, D. L. On the Surface Analysis of Copper Oxides: The Difficulty in Detecting Cu_3O_2. *Vacuum* **2004**, *77*, 27–35.
(7) Hapase, M. G.; Gharpurey, M. K.; Biswas, A. B. The Oxidation of Vacuum Deposited Films of Copper. *Surf. Sci.* **1968**, *9*, 87–99.
(8) Cocke, D. L.; Schennach, R.; Hossain, M. A.; Mencer, D. E.; McWhinney, H.; Parga, J. R.; Kesmez, M.; Gomes, J. A. G.; Mollah, M. Y. A. The Low-Temperature Thermal Oxidation of Copper, Cu_3O_2, and its Influence on Past and Future Studies. *Vacuum* **2005**, *79*, 71–83.
(9) Tretyakov, Yu. D.; Komarov, V. F.; Prosvirnina, N. A.; Kutsenok, I. B. Nonstoichiometry and Defect Structures in Copper Oxides and Ferrites. *J. Solid State Chem.* **1972**, *5*, 157–167.
(10) Huang, T. J.; Tsai, D. H. CO Oxidation Behavior of Copper and Copper Oxides. *Catal. Lett.* **2003**, *87*, 173–178.
(11) Jena, P.; Castleman, A. W. Mass Spectrometry and Its Role in Advancing Cluster Science. *Int. J. Mass Spectrom.* **2015**, in press.

DOI: 10.1021/jp511840d
J. Phys. Chem. C XXXX, XXX, XXX–XXX

(12) Johnson, G. E.; Tyo, E. C.; Castleman, A. W., Jr. Cluster Reactivity Experiments: Employing Mass Spectrometry to Investigate the Molecular Level Details of Catalytic Oxidation Reactions. *Proc. Natl. Acad. Sci. U. S. A.* **2008**, *105*, 18108−18113.
(13) Gord, J. R.; Bemish, R. J.; Freiser, B. S. Collision-Induced Dissociation of Positive and Negative Copper Oxide Cluster Ions Generated by Direct Laser Desorption/Ionization of Copper Oxide. *Int. J. Mass Spectrom. Ion Processes* **1990**, *102*, 115−132.
(14) Irion, M. P.; Selinger, A. Fourier Transform Ion Cyclotron Resonance Studies of Sputtered Metal Cluster Ions: The Chemistry of Cu_n^+ with O_2. *Chem. Phys. Lett.* **1989**, *158*, 145−151.
(15) Ma, C.; Li, H.; Zhang, X.; Bai, J.; Wang, X.; Wang, L.; Zhang, G.; He, G.; Lou, N. Formation of Copper Oxide Cluster Ions - Copper Oxide Cluster Ions Generated by Direct Laser Ablation of Copper Oxide Solid. *Prog. Nat. Sci.* **1996**, *6*, 159−164.
(16) Hirabayashi, S.; Ichihashi, M.; Kondow, T. Reactions of Copper Cluster Cations with Nitrous Oxide: Oxidation and Sequential N_2O Adsorption. *Chem. Phys. Lett.* **2012**, *533*, 15−19.
(17) Hirabayashi, S.; Kawazoe, Y.; Ichihashi, M. CO Oxidation by Copper Cluster Anions. *Eur. Phys. J. D* **2013**, *67*, 35.
(18) Reveles, J. U.; Johnson, G. E.; Khanna, S. N.; Castleman, A. W., Jr. Reactivity Trends in the Oxidation of CO by Anionic Transition Metal Oxide Clusters. *J. Phys. Chem. C* **2010**, *114*, 5438−5446.
(19) Aubriet, F.; Poleunis, C.; Chaoui, N.; Maunit, B.; Millon, E.; Muller, J.; Bertrand, P. Laser Ablation and Static Secondary Ion Mass Spectrometry Capabilities in the Characterization of Inorganic Materials. *Appl. Surf. Sci.* **2002**, *186*, 315−321.
(20) Torres, R.; Jadraque, M.; Martín, M. Cluster Formation and Laser-Induced Effects in the Ablation of $2Cu(CO_3)\cdot Cu(OH)_2$. Time-of-Flight Mass Spectrometric Study. *Appl. Phys. A: Mater. Sci. Process.* **2004**, *79*, 1057−1060.
(21) Matsuda, Y.; Shin, D. N.; Bernstein, E. R. On the Copper Oxide Neutral Cluster Distribution in the Gas Phase: Detection Through 355 and 193 nm Multiphoton and 118 nm Single Photon Ionization. *J. Chem. Phys.* **2004**, *120*, 4165−4171.
(22) Sugawara, K.; Miyawaki, J.; Ikuyama, T.; Arai, I. The Reaction of Copper and Copper Oxide Cluster Cations with NO. *Annu. Meet. Jpn. Soc. Mol. Sci.* **2009**, 2P012.
(23) Cocke, D. L.; Chuah, G. K.; Kruse, N.; Block, J. H. Copper Oxidation and Surface Copper Oxide Stability Investigated by Pulsed Field Desorption Mass Spectrometry. *Appl. Surf. Sci.* **1995**, *84*, 153−161.
(24) Jadraque, M.; Martín, M. DFT Calculations of $Cu_nO_m^{0/+}$ Clusters: Evidence for Cu_2O Building Blocks. *Chem. Phys. Lett.* **2008**, *456*, 51−54.
(25) Wang, L. S.; Wu, H.; Desai, S. R.; Lou, L. Electronic Structure of Small Copper Oxide Clusters: From Cu_2O to Cu_2O_4. *Phys. Rev. B* **1996**, *53*, 8028−8031.
(26) Yin, S.; Bernstein, E. R. Gas Phase Chemistry of Neutral Metal Clusters: Distribution, Reactivity and Catalysis. *Int. J. Mass Spectrom.* **2012**, *321*−*322*, 49−65.
(27) Morita, K.; Sakuma, K.; Miyajima, K.; Mafuné, F. Thermally and Chemically Stable Mixed Valence Copper Oxide Cluster Ions Revealed by Post Heating. *J. Phys. Chem. A* **2013**, *117*, 10145−10150.
(28) Lang, S. M.; Fleischer, I.; Bernhardt, T. M.; Barnett, R. N.; Landman, U. $Pd_6O_4^+$: An Oxidation Resistant yet Highly Catalytically Active Nano-Oxide Cluster. *J. Am. Chem. Soc.* **2012**, *134*, 20654−20659.
(29) Lang, S. M.; Schnabel, T.; Bernhardt, T. M. Reactions of Carbon Monoxide with Free Palladium Oxide Clusters: Strongly Size Dependent Competition between Adsorption and Combustion. *Phys. Chem. Chem. Phys.* **2012**, *14*, 9364−9370.
(30) Himeno, H.; Miyajima, K.; Yasuike, T.; Mafuné, F. Gas Phase Synthesis of Au Clusters Deposited on Titanium Oxide Clusters and Their Reactivity with CO Molecules. *J. Phys. Chem. A* **2011**, *115*, 11479−11485.
(31) Yamada, A.; Miyajima, K.; Mafuné, F. Catalytic Reactions on Neutral Rh Oxide Clusters More Efficient than on Neutral Rh Clusters. *Phys. Chem. Chem. Phys.* **2012**, *14*, 4188−4195.
(32) Sakuma, K.; Miyajima, K.; Mafuné, F. Oxidation of CO by Nickel Oxide Clusters Revealed by Post Heating. *J. Phys. Chem. A* **2013**, *117*, 3260−3265.
(33) Schramm, L.; Behr, G.; Löser, W.; Wetzig, K. Thermodynamic Reassessment of the Cu−O Phase Diagram. *J. Phase Equilib. Diffus.* **2005**, *26*, 605−612.
(34) Vann, W. D.; Bell, R. C.; Castleman, A. W., Jr. Gas-Phase Reactions of Nickel and Nickel Oxide Clusters with Nitrogen Oxides. 3. Reactions of Cations with Nitric Oxide. *J. Phys. Chem. A* **1999**, *103*, 10846−10850.
(35) Ferrandon, M.; Carnö, J.; Järås, S.; Björnbom, E. Total Oxidation Catalysts Based on Manganese or Copper Oxides and Platinum or Palladium I: Characterisation. *Appl. Catal., A* **1999**, *180*, 141−151.
(36) Hirabayashi, S.; Ichihashi, M. Reactions of Size-Selected Copper Cluster Cations and Anions with Nitric Oxide: Enhancement of Adsorption in Coadsorption with Oxygen. *J. Phys. Chem. A* **2014**, *118*, 1761−1768.

DOI: 10.1021/jp511840d
J. Phys. Chem. C XXXX, XXX, XXX−XXX